

1 Water sorption and diffusion in cellulose acetate: the effect of plasticisers

2 Isabella del Gaudio¹, Elwin Hunter-Sellars², Ivan P. Parkin³, Daryl Williams^{2,4}, Simoní Da Ros¹,
3 Katherine Curran¹

4 ¹Institute Sustainable Heritage, University College London, 14 Upper Woburn Place London WC1H
5 ONN, United Kingdom

6 ²Department of Chemical Engineering, Imperial College London, Exhibition Road, Kensington, London
7 SW7 2AZ, United Kingdom

8 ³Faculty of Maths & Physical Sciences, University College London, Gower St, Bloomsbury, London
9 WC1E 6BT, United Kingdom

10 ⁴Surface Measurement Systems Ltd. Unit 5, Wharfside Rosemont Road Alperton, London, HA0 4PE,
11 United Kingdom

12 Keywords: cellulose acetate, water sorption, water diffusion, plasticiser loss

13 Abstract

14 The conservation of cellulose acetate plastics in museum collections presents a significant challenge,
15 due to the material's instability. Several studies have led to an understanding of the role of relative
16 humidity (RH) and temperature in the decay process. It is well established that the first decay
17 mechanism in cellulose acetate museum objects is the loss of plasticiser, and that the main decay
18 mechanism of the polymer chain involves hydrolysis reactions. This leads to the loss of sidechain
19 groups and the breakdown of the main polymer backbone. However, interactions between these
20 decay mechanisms, specifically the way in which the loss of plasticiser can modify the interaction
21 between cellulose acetate and water, has not yet been investigated. This research addresses the role
22 of RH, studying the sorption and diffusion of water in cellulose acetate and how this interaction can
23 be affected by plasticiser concentration using Dynamic Vapour Sorption (DVS).

24 1 Introduction

25 Water sorption and diffusion have been a subject of
26 interest in many different research areas including
27 membrane separation, pharmacology, food packaging
28 and fibres as well as material degradation (Allada et al.,
29 2017; Argyropoulos et al., 2011; Céline et al., 2014;
30 Kohler et al., 2003; Kurokawa, 1981; Kymäläinen et al.,
31 2015; Leão & Tuller, 2014; Zhang et al., 2013).
32 Materials can be affected by the relative humidity (RH)
33 of the environment, which can often cause
34 undesirable changes in mechanical and chemical
35 properties. Furthermore, it is particularly concerning in
36 museum institutions where, due to the rarity of
37 artefacts, control of environmental factors such as
38 temperature and RH are needed to slow down
39 degradation processes (Wäntig, 2008). Due to the lack
40 of international standards for storage of plastic
41 artefacts in museums, it is not uncommon for
42 museums to apply the same environmental
43 parameters used for classic heritage organic materials

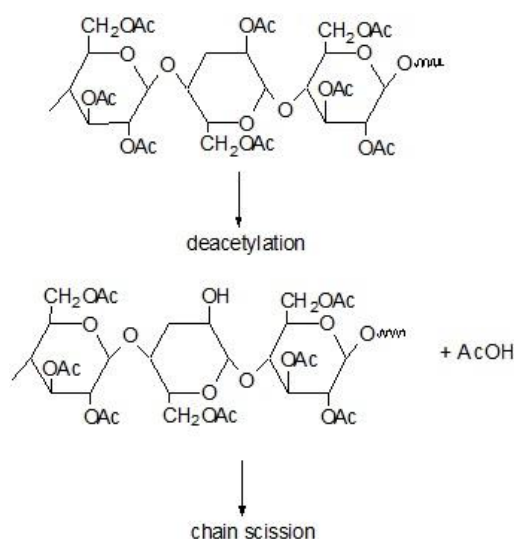


Figure 1: Schematic representation of hydrolysis steps in cellulose acetate. The first step, deacetylation, causes the substitution of acetate (Ac) by hydroxyl groups with the consequent emission of acetic acid. The second step known as chain scission causes the cleavage of glycosidic group.

44 (e.g. paper) to plastics and to store them at 18-20 °C and 50% RH (Shashoua, 2014).

45 In cellulose acetate, hydrolysis is an intensively studied, complex subject in the life-assessment and
46 decay mechanism of archival materials and plastics (Allen et al., 1987, 1987; Edge et al., 1989; Edwards
47 et al., 1993; Littlejohn et al., 2013, 2013; McGath, 2012; Wäntig, 2008; Shashoua, 2008), with a variety
48 of chemical and physical mechanisms involved. Cellulose acetate spontaneously undergoes hydrolysis
49 (enhanced by high temperatures and RH) losing acetic acid and causing a decrease of the degree of
50 substitution (DS), the mechanism of which is shown in Figure 1 (deacetylation). This process is known
51 as vinegar syndrome for the strong smell of acetic acid produced during the decay mechanism, an
52 autocatalytic reaction that decreases the pH and consequently accelerates the ageing process (Edge
53 et al., 1989). The trapped acid can catalyse the hydrolysis of C-O bonds in the polymer backbone,
54 reducing the length of the polymer chain (Ballany et al., 2000) in a process known as chain scission. In
55 a study carried out by Allen et al. (1987) water absorption in film originally stored in cans seems to be
56 one of the most important parameters for controlling cellulose acetate film decay. The results showed
57 that the absorption of water accelerates hydrolytic degradation, promoting the emission of acetic acid
58 which itself will catalyse the decay process.

59 Many cellulose acetate objects contain plasticisers which are added to the polymer matrix to confer
60 flexibility and malleability thanks to their ability to reduce polymer-polymer secondary interactions
61 and the polymer's crystallinity (Brydson, 1999). Diethyl Phthalate ($C_{12}H_{14}O_4$) was one of the main
62 plasticisers (Brydson, 1999) used historically in cellulose acetate however, due to its impact on the
63 flammability of the polymer (Brydson, 1999) Triphenyl Phosphate ($C_{18}H_{15}O_4P$) was also added as a
64 flame retardant (Brydson, 1999). The migration and evaporation of plasticisers into the surrounding
65 environment during ageing is a well-documented phenomenon (Godwin, 2017; Richardson et al.,
66 2014; Shashoua, 2008) and Ballany et al. (2000) have identified the loss of plasticiser as the first decay
67 mechanism that occurs in cellulose acetate artefacts followed by deacetylation and finally chain
68 scission.

69 Cellulose acetate, being a biodegradable polymer and due to its excellent optical clarity and high
70 toughness (Park, Liang, et al., 2004; Rhim & Ng, 2007; Sharma et al., 2021) has found applications as
71 cigarette filters, photographic base material, membranes, medical implants and currently, in food
72 packaging. However, due to its brittleness and water sensitivity, reinforcing materials are generally
73 added. Current research is investigating the effect of fillers such as nanocomposites (Kalaycioğlu et al.,
74 2020; Park, Liang, et al., 2004; Park, Misra, et al., 2004) and cellulose nanofibers (Sharma et al. 2021)
75 on cellulose acetate films to improve their mechanical and thermal properties and permeability. In
76 general, moisture content, water vapour transport, permeability and swelling decrease with increased
77 quantities of fillers, which can be caused by the formation of strong hydrogen bonds between polymer
78 and filler (Rhim & Ng, 2007; Sharma et al., 2021) or by the nanocomposites acting as obstacles and
79 creating a tortuous path for gas molecules to penetrate cellulose acetate. Park, Misra, et al., (2004)
80 also observed the effect of plasticisers with an increase in permeability with higher amounts of
81 plasticisers.

82 The majority of the works on sorption and diffusion of water in cellulose acetate have been carried
83 out on membranes and often to investigate the effect of DS (Kurokawa, 1981; Lonsdale et al., 1965;
84 D. Murphy & de Pinho, 1995; Palin et al., 1975; Roussis, 1981b, 1981a; Zhang et al., 2013), similar
85 studies on plasticised cellulose acetate are less common. Works by Keely et al. (1995) and Scandola &
86 Ceccorulli (1985) observed that increased plasticiser concentration reduced the amount of water
87 absorbed by cellulose acetate, but this was not investigated as a function of relative humidity. Studies
88 of the impact of plasticiser concentration on the diffusion of water in cellulose acetate are also lacking.
89 It could be hypothesised that the enhancement in polymer mobility caused by increased plasticiser

90 concentration could increase the rate of diffusion of water. However, a study carried out by
91 Belokurova et al., (2004) on cellulose acetate plasticised with Dimethyl Phthalate and Dibutyl
92 Phthalate found that plasticiser concentrations lower than 20% in fact reduced the rate of diffusion of
93 water into the polymer. The authors speculated that at lower concentrations plasticisers are not
94 organised within the polymer's interchain regions and instead act as obstacles to the water's migration
95 pathways, while at plasticiser concentrations above 20% 'effective plasticisation' take place. However,
96 the authors conducted no further tests to prove this hypothesis.

97 In this work we explore the interaction between water vapour and plasticised cellulose acetate using
98 Dynamic Vapour Sorption (DVS). DVS has been used to measure the interactions of water vapour with
99 fibres (Okubayashi et al., 2004; Xie et al., 2011), archival materials (Popescu et al., 2016)
100 pharmaceuticals (Rajabnezhad et al., 2020), and various porous materials (Hunter-Sellers et al., 2020).
101 This gravimetric technique allows the study of water vapour sorption and diffusion under realistic
102 storage conditions comparable to those adopted by the museums (20 °C). We investigated the
103 hydrophobicity that plasticisers introduce to the material and its influence on water- cellulose acetate
104 interactions as a function of RH levels.

105 This vapour-solid interaction is also influenced by the volatility of the plasticisers. To this end, we
106 investigated the loss of diethyl phthalate and triphenyl phosphate from cellulose acetate films at
107 different RHs and temperatures. The conditions in this study are significantly less extreme than those
108 in previous works (Kovačić & Mrklič, 2002; Mrklič et al., 2004; G.-L. Wei et al., 2015; X.-F. Wei et al.,
109 2019), and much closer to that of real-world storage conditions.

110 **2 Materials and Methods**

111 **2.1 Materials**

112 All materials were used as received. Cellulose acetate samples were prepared by dissolving 0.5 g of
113 commercial cellulose acetate (Sigma Aldrich, Mn 30,000, assay \geq 99.5%) in 100 mL of acetone (Sigma
114 Aldrich, 99.5% purity) with either 10 or 20 wt.% diethyl phthalate (99.5% purity, purchased from Sigma
115 Aldrich) or triphenyl phosphate (99% purity, purchased from Sigma Aldrich) (Figure S1 in
116 Supplementary Information -SI- document). The mixture was refluxed for 2 h and then cooled for 1 h,
117 both under constant stirring. Afterwards, the mixture was poured over a glass dish 26 cm in diameter
118 and covered with a glass lid. After a week of slow evaporation at room temperature, the cellulose
119 acetate films were placed separately in a vacuum oven at room temperature and 150 mbar to dry for
120 two weeks to avoid cross contamination.

121 The final thickness of the samples was approximately 15 μm . All the samples were stored in the fridge
122 at 5 °C before use.

123 **2.2 Methods**

124 **2.2.1 Artificial ageing**

125 Approximately 50 mg of sample was placed in a 100 mL Duran bottle hanging using a stainless-steel
126 filament and aged using a saturated solution of sodium bromide as illustrated in Figure S2 in the SI
127 document. The bottles were placed for two months in an oven at a temperature of 70 °C and an RH of
128 approximately 50% for two months.

129 **2.2.2 ATR-IR spectroscopy**

130 A Bruker Alpha spectrometer with a Platinum ATR single reflection diamond as Internal Reflection
131 Element (IRE) accessory attached was used. The analysis was performed over a wavenumber range of
132 400-4000 cm^{-1} , using a wavenumber resolution of 4 cm^{-1} and 32 scans and the spectra of the samples

133 were collected in absorbance mode. A background spectrum was collected under the same conditions
134 before analysis. The spectra were recorded using *OPUS* software and the resulting spectra were
135 processed using *Origin Pro* software.

136 The alteration in plasticiser concentration was determined through the plasticiser-to- cellulose
137 acetate intensity ratio. The CH benzene band at 748 cm⁻¹ and 778 cm⁻¹ was selected to monitor diethyl
138 phthalate and triphenyl phosphate respectively, and they were normalised against the peak at 602
139 cm⁻¹, corresponding to the C-C-C backbone of the cellulose ring (Gautam et al., 2016; Richardson et
140 al., 2014; Skorniyakov & Komar, 1998). This peak has been considered the internal standard, a constant
141 that is unaffected by the concentration of plasticiser and the hydrolysis process (Richardson et al.,
142 2014). The baseline of the spectrum was corrected by averaging the intensity between 2000 and 2200
143 cm⁻¹ and subtracting this value from the intensity at every wavenumber.

144 2.2.3 ¹H NMR spectroscopy

145 For all NMR analyses, deuterated dimethyl sulfoxide (DMSO-d₆, 99.9 atom % D, Sigma Aldrich,
146 London, United Kingdom, used as received) was used as the solvent. DMSO-d₆ has been selected as
147 a solvent able to dissolve cellulose acetate with a DS between 0.5 and 2.9 (Cao et al., 2010). The ¹H
148 NMR experiments were performed at 298 K using a Bruker Avance Neo NMR spectrometer operating
149 at 700 MHz and equipped with a helium-cooled broadband cryoprobe, using a standard single pulse
150 experiment with a 30° pulse (zg30 in the standard library of Bruker NMR pulse sequences). The
151 acquisition time and relaxation delay were equal to 4 and 50 s, respectively, and the number of scans
152 was equal to 64. Fourier transformation was performed using the exponential window function with
153 line broadening factor equal to 0.3 Hz, followed by phase and baseline correction using the TopSpin
154 software, version 4.0.3. Triplicates have been performed for each sample. The chemical shifts in the
155 NMR data were calibrated by assigning the DMSO-d₆ solvent residual peak as 2.50 ppm. The
156 procedure used is similar to the one described by Da Ros et al. (2020).

157 Between 3-10 mg of sample was placed in sealed glass vials and dissolved in 2 mL of DMSO-d₆ in an
158 ultrasonic bath for 30 min at room temperature to avoid loss of plasticisers. 650 µL of solution was
159 placed in another vial, adding 150 µL of an internal standard solution (104.5 mgmL⁻¹ of 1,2,4,5-
160 tetrachloro-3-nitrobenzene (99.82%, Sigma Aldrich)). The final solution was transferred to a 5 mm
161 NMR tube.

162 The diethyl phthalate concentration (in wt%) was determined using the following equation:

$$163 \text{ Plasticiser content (\%)} = \frac{I_{PL}}{I_{IS}} \frac{N_{IS}}{N_{PL}} \frac{M_{PL}}{M_{IS}} \frac{m_{IS}}{m_S} P_{IS} \quad (1)$$

164 where I_{PL} and I_{IS} are the integrated areas of plasticiser (PL) and internal standard (IS) peaks respectively,
165 N represents the number of ¹H nuclei that correspond to those peaks; M is the molecular mass in
166 g·mol⁻¹ of the compound; m represent the mass of sample (S) and internal standard (IS) used in the
167 analysis and, finally, P denotes the IS mass fraction purity which in this work is 99.82%.

168 I_{PL} refers to the integrated area of the diethyl phthalate methyl triplet which is calculated between
169 1.40 and 1.15 ppm for samples in which diethyl phthalate was used as the plasticiser, or the integrated
170 area of the peaks between 7.50 and 7.20 ppm for samples in which triphenyl phosphate was used as
171 the plasticiser while I_{IS} refers to the integrated area of the Internal Standard (IS) singlet resonance,
172 calculated between 8.57 and 8.37 ppm; N for the diethyl phthalate, triphenyl phosphate and IS
173 molecules are equal to 6, 15 and 1 respectively.

174 2.2.4 Solid Phase Micro Extraction GC-MS

175 The volatiles emitted by plastics, such as plasticisers, can be analysed by SPME-GC/MS. The same
176 method as described by Curran et al. (2016) was used. Before proceeding with the analysis of VOCs, 1
177 mL of standard solution was placed in a 20 mL Chromacol headspace sample vial (20-HSV T229) and
178 sealed with a Chromacol 18mm Magnetic Screw Cap with a 1 mm Silicone/PTFE Liner - Not Prefitted
179 (18-MS-SC101). The standard solution was a MISA Group 17 Non-Halogen Organic Mix purchased
180 from Sigma Aldrich (48133 Supelco). It contains 2000 µg/ml each of
181 benzene, ethylbenzene, styrene, toluene and ortho-, meta- and para-xylene in methanol and 1 mL of
182 solution was diluted up to 50 mL in methanol. A sampling time of 20 s at room temperature was
183 performed using a 50/30 µm DVB/CAR/PDMS fibre (purchased from Sigma Aldrich), manually injected
184 into the port of a gas chromatograph (Perkin Elmer Clarus 500) to a mass spectrometer (Perkin Elmer
185 Clarus 560D). The column used was a coiled VOCOL (Supelco, 20% phenyl–80% methylpolysiloxane)
186 60 m in length and 0.25 mm in diameter. The temperature was increased by 10 °Cmin⁻¹ from 35 °C up
187 to 200 °C and it was held for 10 min. The carrier gas was helium with a constant flow of 1 mLmin⁻¹. The
188 DVB/CAR/PDMS fibre provides larger qualitative distribution of VOCs (Lattuati-Derieux et al., 2013)
189 with molecular weights between 30 and 225.

190 Samples were inserted into a 20 mL Chromacol headspace sample vial. VOC analysis was performed
191 using the method described by Curran et al., (2016). The fibre was kept for five days into a Chromacol
192 headspace sample vial and then manually injected into the port of a gas chromatograph. The following
193 heating program was used: an initial temperature of 50 °C was held for 5 min, increased with a ramp
194 rate of 10 °Cmin⁻¹ to 100 °C, then 5 °Cmin⁻¹ to 200 °C and 2 °Cmin⁻¹ to 220 °C (held for 20 min). The
195 injector temperature was 250 °C. The interface and source temperatures were 200 °C and 180 °C
196 respectively. Mass spectra were collected under electron ionization (EI) mode at 70 eV and recorded
197 from m/z = 45–300. The same method was performed using a blank fibre to act as a background. The
198 identification of peaks was performed using the NIST 2005 Mass Spectra Library V2.1.

199 During VOCs extraction the environment was monitored using a HOBO data logger recording 21.74 ±
200 0.26 °C and 50 ± 3.40% RH with an accuracy of ± 0.2 °C and ± 2.5% RH.

201 2.2.5 Contact angle

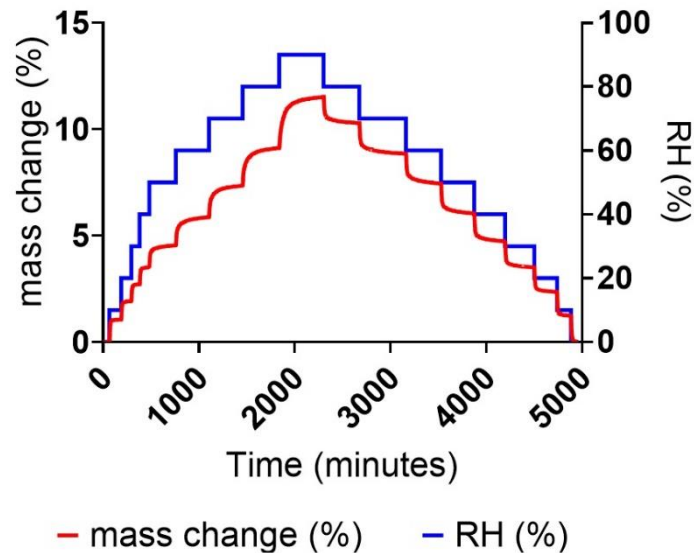
202 Water contact angle for cellulose acetate films with and without plasticisers was calculated using an
203 FTA-1000B (First Ten Angstroms, Inc.) setup and FTA32 software. The films were placed on glass and
204 taped on the side to keep them fixed and flat throughout the experiment. Deionized water was added
205 to a 1 ml gastight Hamilton syringe and a 6±0.5 µL drop was placed directly above the sample. Using
206 the FTA32 software, a video capture was initiated, and a single drop of water released. An image was
207 captured every 0.1 s until the drop reached a static position (10 s). The contact angle, diameter,
208 volume and area were measured throughout the film. Five measurements on different spots were
209 performed for each sample and the mean of left and right angle was used for the calculations.

210 The environment was monitored using a HOBO data logger recording 25.8 ± 1.8 °C and 55 ± 3.70% RH
211 with an accuracy of ± 0.2 °C and ± 2.5% RH.

212 2.2.6 Dynamic Vapour Sorption (DVS)

213 Water vapour isotherms for non-plasticised and plasticised cellulose acetate were measured using a
214 DVS Endeavour (Surface Measurement Systems, UK). For each experiment samples weighing
215 approximately 30-50 mg were placed onto high sensitivity balances and exposed to varying levels of
216 water vapour via a bubbling system. Samples were dried by passing over dry air at 20 °C until the
217 sample masses remained constant. In all isotherm experiments, the samples were dried by holding
218 at atmospheric pressure, 20 °C, and using a dry air flowrate of 200 mL min⁻¹. Samples were then

219 exposed to humidity values from 0-90% in 10% increments, with the equilibrium mass determined
 220 once the mass vs time gradient reached a value no greater than 0.0005 dry mass % per minute.
 221



222
 223 *Figure 2: An example of a sorption kinetic graph used to calculate D.*

224 Dynamic vapour sorption was also utilised for measuring the loss of plasticiser when samples were
 225 exposed to several temperatures and RH combinations (20, 30, and 40 °C at constant 50% RH and 25,
 226 50, and 75% RH at a constant temperature of 30 °C). For each experiment, the samples were dried as
 227 described above, although at the chosen temperature, before being exposed to a particular RH and
 228 held at that RH for minimum of 720 minutes.

229 To understand how water diffuses within the polymer matrix during RH fluctuations in museum
 230 environments, the water diffusion coefficient (*D*) was modelled at each RH stage of the real time
 231 sorption kinetics graph as illustrated in Figure 2 (Preda et al., 2015) using the following equation
 232 (Barham et al., 2015; Crank, 1975):

233
$$\frac{M_t}{M_\infty} = \frac{4}{d} * \sqrt{\frac{Dt}{\pi}} \quad (2)$$

234 Where *M_t* is the mass at time *t*, *M_∞* is the mass acquired at the thermodynamic equilibrium, *d* is the
 235 thickness of the sample, and *D* is the diffusion coefficient. This is a simplification of the solution to the
 236 diffusion equation for diffusion in a plane sheet at short times. The equation is valid when *M_t* / *M_∞*
 237 ≤ 0.4 (Crank, 1975).

238 **2.2.7 Scanning Electron Microscope (SEM)**

239 Surface films were examined using a Hitachi S-3400N scanning electron microscope (Hitachi, Japan).
 240 A thin gold layer coating was sputtered twice onto the surface to improve sample conductivity. The
 241 accelerating voltage of the SEM was set at 5 kV, and the samples were examined at a working
 242 distance of 8 mm.

243

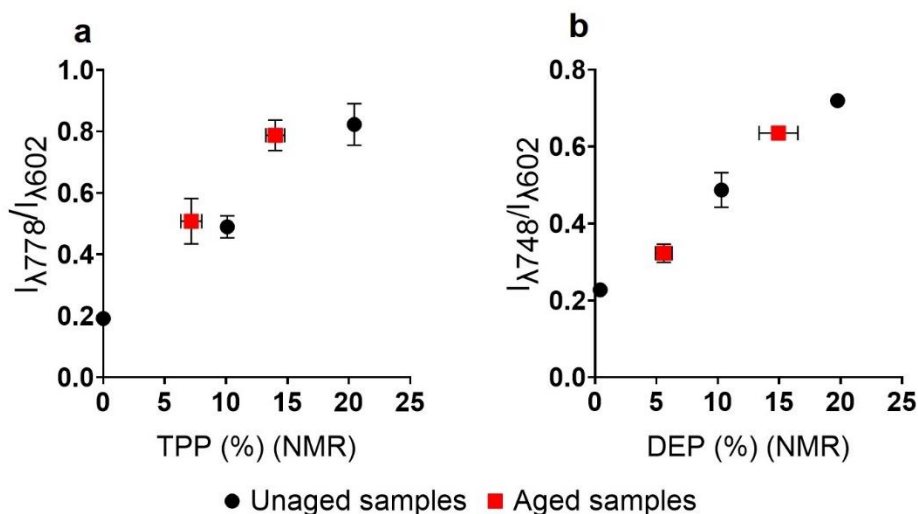
244 **3 Results and discussion**

245 The following sections describe the composition of the aged materials, the insights provided by DVS
246 analysis into the sorption and diffusion of water in cellulose acetate at different RHs and the kinetics
247 of diethyl phthalate loss from cellulose acetate.

248 **3.1 Aged Materials**

249 The aged materials did not show significant changes in their degree of substitution (DS), ranging from
250 2.45 ± 0.02 for non-aged to 2.43 ± 0.01 for aged samples (calculated in accordance to Da Ros et al.
251 (2020), data not shown) and molecular weight (data not shown) but they did present evidence of
252 plasticiser loss.

253 In this work ATR-FTIR analysis has been employed to get indicative information of plasticiser
254 concentration at the sample surface, while ^1H NMR spectroscopy was used for plasticiser
255 quantification (Figure 3). Cellulose acetate film plasticised with diethyl phthalate show a plasticiser
256 reduction of ~5% after aging by both ATR-FTIR and ^1H NMR analysis. This means that samples which
257 initially contained 20 and 10 wt% diethyl phthalate contained 15 and 5 wt% after aging respectively.
258 On the other hand, the films plasticised with triphenyl phosphate do not show the same correlation
259 between ATR-FTIR and ^1H NMR results. While the ATR-FTIR analysis suggests an increase of the
260 plasticiser concentration, the ^1H NMR analysis shows a reduction of the plasticiser concentration
261 (Figure 3b). The increase of the signal from the ATR-FTIR analysis might be caused by the migration of
262 triphenyl phosphate to the surface during ageing (Macro, 2019; Takahashi et al., 2021) as this is a
263 technique for surface analysis, while ^1H NMR spectroscopic analysis measures the plasticiser
264 concentration throughout the bulk of the sample.



265

266 *Figure 3: (a) diethyl phthalate (DEP) concentration and (b) triphenyl phosphate (TPP) concentration of cellulose*
267 *acetate film. On the x-axis are reported the results of ^1H NMR (bulk analysis) and on the y-axis the results of ATR*
268 *(surface analysis).*

269

270 3.2 Contact angle, sorption and diffusion of water

271 3.2.1 Contact angle

272 Surface hydrophobicity has been used as an important indicator in the study of moisture transfer in
273 polymer films. It is usually evaluated by the contact angle between the film surface and a water
274 droplet. Water contact angle increases with increasing surface hydrophobicity. Generally, we can
275 observe that cellulose acetate films are hydrophilic materials having a contact angle below 90°,
276 however with higher plasticiser content there is an increase in contact angle (Figure 4a), indicating
277 that plasticisers have hydrophobic properties. Moreover, SEM images (Figure S3) have indicated no
278 morphological changes on the surfaces as a result of plasticisers addition.

279 The evolution of a drop on a polymeric film can be driven by different mechanisms such as absorption,
280 spreading, swelling and evaporation (Farris et al., 2011; Karbowski et al., 2006; Kokoszka et al., 2010;
281 Modaressi & Garnier, 2002; Solaro et al., 2010). For the films used in this study, the water drop profile
282 changes immediately after deposition onto the film surface (Figure 4). Perceptible changes in
283 diameter, volume and area are observed. Figure 4 clearly shows two stages of the variation of the
284 contact angle. Firstly, there is an initial decrease in contact angle correlated to a reduction in volume
285 (Figure 4b) and an increase of the drop base diameter (Figure 4c). In the second stage, the diameter
286 becomes stable, with the contact angle reaching an equilibrium. Furthermore, the reduction of the
287 drop volume without a corresponding change of area (Figure 4d) suggests that absorption is the
288 prevailing phenomenon on contact angle change (Farris et al., 2011; Karbowski et al., 2006; Modaressi
289 & Garnier, 2002). Recorded initial and final contact angles with respective illustrative images are
290 summarised in Table S1 and S2.

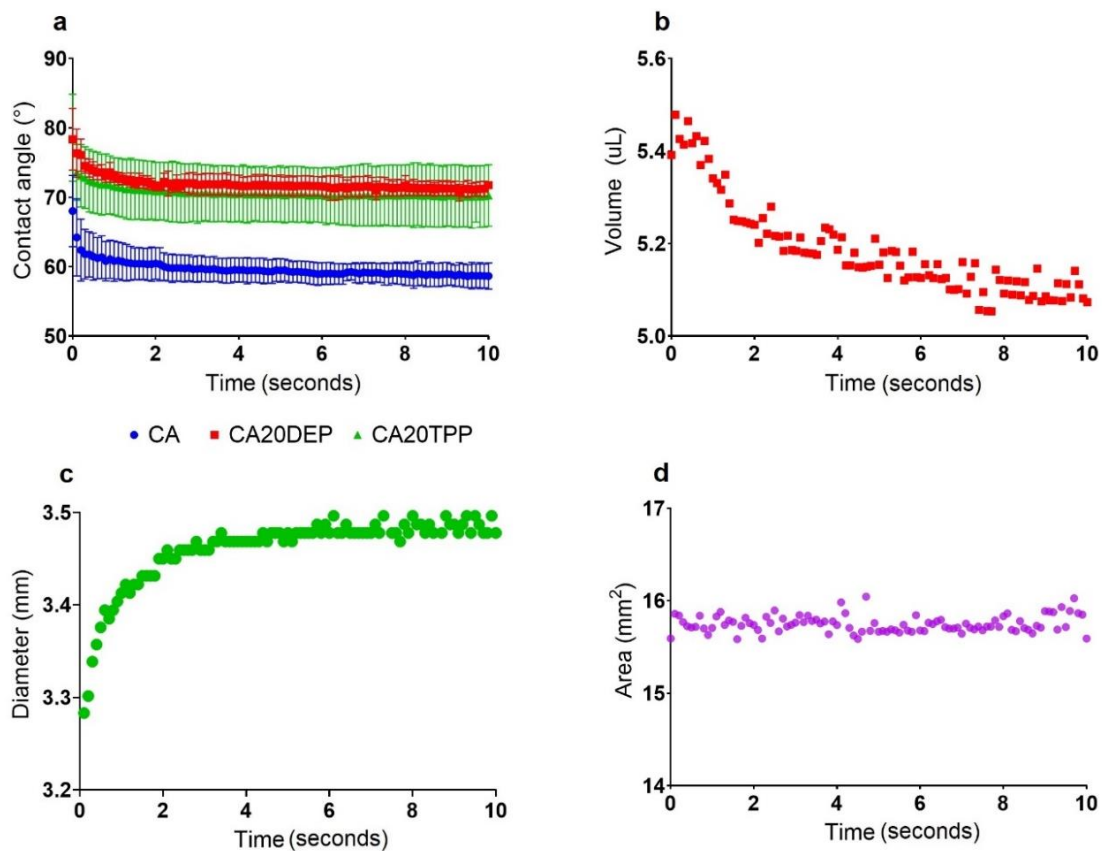


Figure 4:(a) Mean contact angle of unplasticised cellulose acetate (●) and cellulose acetate with 20wt% DEP (■) and TPP (▲). Error bars represent the standard deviation from five water drops' contact angles at each 0.1 s; (b), (c), (d) Typical dynamics of water drop volume, diameter and area observed on films (from 20DEP sample). Each data point represents 0.1 s.

291 Change in contact angle has previously been described using a simple exponential decay function
 292 (Farris et al., 2011). According to Asai et al. (2001), water is absorbed by cellulose acetate through two
 293 distinct processes. One mechanism is associated with the free volume of the polymer and the other
 294 involves cellulose acetate's hydroxyl groups.

295 Considering that the change in contact angle over time appears to be mostly due to absorption rather
 296 than spreading and that it depends on two absorption process, the equation used by Oberbossel et al.
 297 (2016), Eq. (3), who also described two distinct absorption processes, was fitted to the experimental
 298 data. In this equation, $\theta(t)$ represents the contact angle measured at each recording time t and θ_{sat} ,
 299 A_1 , τ_1 , A_2 and τ_2 are the adjustable parameters which were estimated from the experimental
 300 measurements.

$$301 \quad \theta(t) = \theta_{sat} + A_1 \cdot \exp(-t/\tau_1) + A_2 \cdot \exp(-t/\tau_2) \quad (3)$$

302 Table S3 (in the supplementary document) shows these parameters. The good fit obtained, as
 303 illustrated by high determination coefficients, r^2 , Table S3, indicates that the function used is
 304 appropriate and that the decrease in water contact angle, represented by A_1 and A_2 , respectively,
 305 can be caused by the above-mentioned dual absorption process.

306 3.2.2 Sorption and diffusion of water: Isotherm analysis

307 Generally, all samples show that with the increase of RH the water content increases. Furthermore,
 308 the DVS results show that plasticisers have a hydrophobic effect and therefore, with an increase in

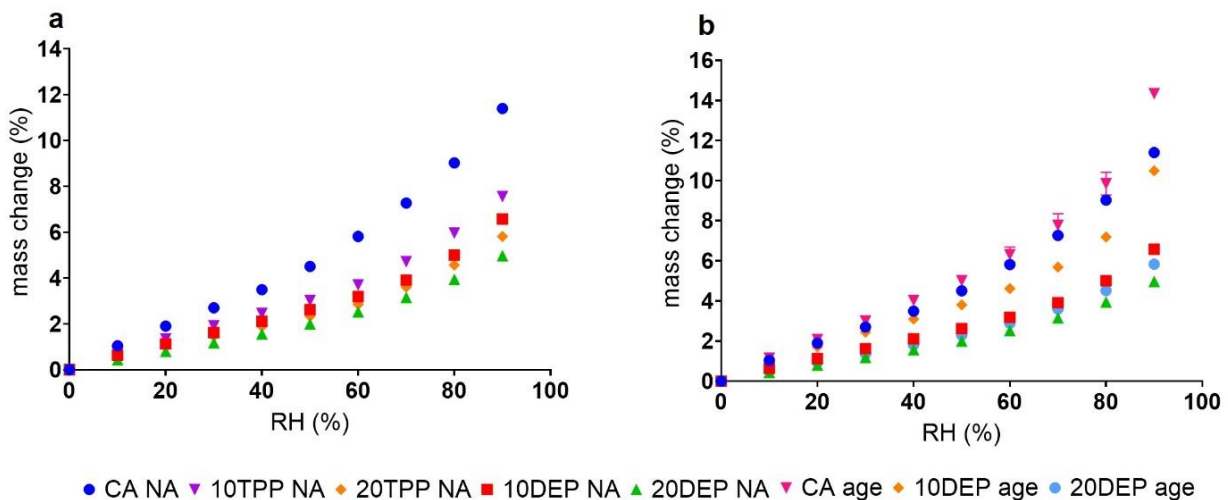


Figure 5(a) Isotherm plot of unaged (NA) cellulose acetate (CA) film plasticised with diethyl phthalate (DEP) and triphenyl phosphate (TPP) at 10 or 20 wt%. (b) Isotherm plot of aged and NA film plasticised with DEP.

309 plasticiser concentration, the cellulose acetate absorbs less water as shown in Figure 5a. It has been
 310 previously observed that with an increase of diethyl phthalate cellulose acetate absorbed less water
 311 (Keely et al., 1995; Scandola & Ceccorulli, 1985). Keely et al. (1995) proposed that this was because
 312 the presence of diethyl phthalate led to a reduction in the number of available hydrophilic groups to
 313 interact with water via hydrogen bonding. A summary of sorption values of the cellulose acetate film
 314 is reported in Tables S4-S5 in the SI document. With the increase of diethyl phthalate concentration,
 315 water regain decreases from 11.40% (un-plasticised cellulose acetate) to 4.97% (20 wt% diethyl
 316 phthalate) at 90% RH (Table S4).

317 Aged samples showed greater water affinity than non-aged samples for those containing plasticiser
318 (Figure 5b). This is likely due to the loss of plasticiser during aging. Non-plasticised cellulose acetate
319 showed a small increase in water uptake following aging, which became more significant at higher RH,
320 suggesting that aging resulted in some changes to even the non-plasticised samples' sorption
321 properties. However, considering the large difference in water affinity between aged and non-aged
322 10% diethyl phthalate samples, with uptake almost doubling (6.58% for unaged and 10.49% for aged
323 sample) at 90% humidity (Table S5), plasticiser loss is likely a significant contributor to sample
324 hydrophilicity. This relationship has been observed with the contact angle as well where plasticised
325 samples show an increase of the water drop contact angle, indicating increased hydrophobicity (Table
326 S1).

327 The repeatability of the analysis has been carried out on both aged cellulose acetate and aged samples
328 with an initial 20 wt% diethyl phthalate concentration. While it is unclear if the increase of water
329 sorption is affected by DS in this work, the difference between un-plasticised and plasticised samples
330 is clear.

331 Data from the isotherms were fitted in the data range of 10-90% RH using the Guggenheim-Anderson-
332 de Boer (GAB) and Brunauer-Emmett-Teller (BET) equations (Alamri et al., 2018). The goodness of fit
333 was evaluated using the root-mean-square error (RMSE). A summary of fitting parameters is provided
334 in Table S6 (supplementary document). Experimental data were best described by the GAB model and
335 a good fit was found up to 60% RH, whereas at higher humidity both BET and GAB models
336 overestimate the water uptake as shown in Figure S4.

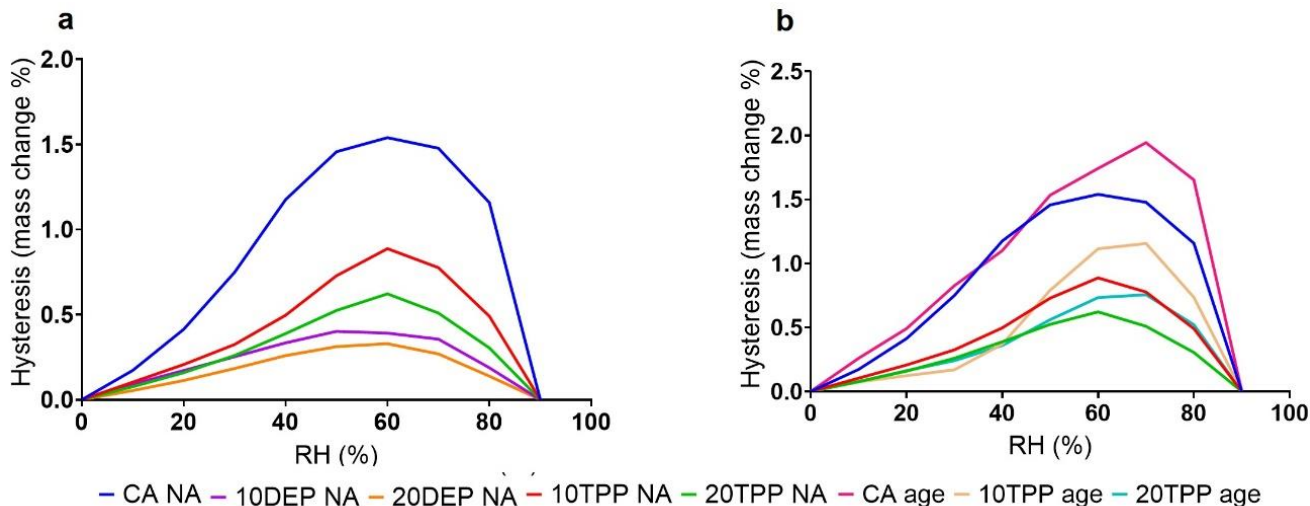
337 A mathematical function was fitted to the experimental mass change (MC) values collected at different
338 RH with the goal of obtaining an analytical expression that defines how MC changes based on RH and
339 plasticiser content (Pl). The relationship between MC and RH results in a polynomial of 3rd order while
340 the relationship between MC and plasticiser content (either DEP or TPP content expressed as wt%) is
341 described by a 2nd order polynomial (Figure S5a, supplementary document). The data has been fitted
342 using Origin 2020b (OriginLab, USA). The resulting calibration equation of MC with RH and plasticiser
343 content for both the sorption and desorption processes has been presented as:

$$344 \quad MC = a + b \cdot RH + c \cdot Pl + d \cdot RH^2 + e \cdot Pl^2 + f \cdot RH^3 + g \cdot RH \cdot Pl + h \cdot RH^2 \cdot Pl + i \cdot RH \cdot Pl^2 \quad (4)$$

345 Estimated coefficients are presented in Table S7 in the supplementary document. For the equation
346 fitting, data from aged samples were included as well, as the DS change was not considered significant
347 (from 2.45 ± 0.02 to 2.43 ± 0.01 for non-aged and aged samples, respectively). An example of the
348 trend of the 3D data points is shown in Figure S5b. While this relationship can be helpful for
349 quantifying and understanding how MC changes as a function of RH and plasticiser content, further
350 studies are needed to validate the relationship.

351 3.2.3 Sorption and diffusion of water: Hysteresis

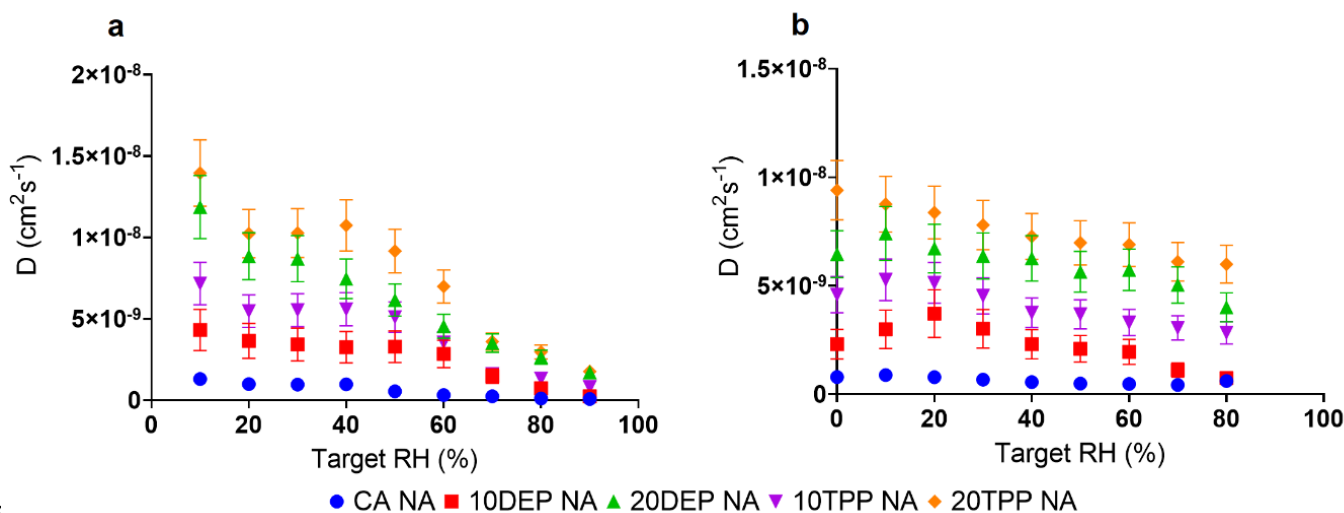
352 Generally, the isotherm plot shows that at the same RH, the sample contains more water during
353 desorption. Plotting hysteresis (given by the difference in water content during the sorption and
354 desorption processes) vs RH we can notice that hysteresis has a peak around 60% RH (Figure 6).
355 Furthermore, with the increase in plasticiser concentration, hysteresis decreases. Analysis of the
356 hysteresis suggests that it is caused by the polymer-water interactions via hydrogen bonding, which
357 are interrupted by the presence of plasticiser, as proposed by Chen et al. (2018). Hence, it can be
358 expected that the reduced hysteresis is caused by the reduction of active sites for polymer-water
359 hydrogen bonding. Aged cellulose acetate films show an increase of hysteresis mainly due to loss of
360 plasticiser although it can be supposed that the decrease in DS (although minor in our aged samples)
361 which causes an increase of hydroxyl groups, could have some significance as well.



363
 364 *Figure 6: Hysteresis plot vs RH of (a) Unaged (NA) cellulose acetate (CA) films at different plasticiser content and*
 365 *(b) after ageing.*

366 **3.2.4 Sorption and diffusion of water: diffusion coefficients of water in cellulose acetate**

367 In this work, the values of the diffusion coefficients (D) of water vary from 1.3×10^{-9} to $1.45 \times 10^{-8} \text{ cm}^2 \text{ s}^{-1}$
 368 ¹. The values measured in this work are similar to previous studies where the rate of the sorption was
 369 monitored by measuring the elongation of the quartz springs in a sorption chamber at 25°C (Roussis,
 370 1981a). Roussis (1981b) found the D of cellulose acetate membranes to be of the order of $1.2\text{-}8.2 \times 10^{-8}$
 371 $\text{cm}^2 \text{ s}^{-1}$. Belokurova et al., (2004) have calculated the D of water in plasticised cellulose acetate film
 372 (from 0 to 47 wt% of plasticiser with thickness between 0.002 and 0.005 mm) using a McBain balance.
 373 However, the results obtained by Lonsdale et al. (1965) are substantially different, the D value of
 374 cellulose acetate membrane with 39.8% acetyl content at 100% RH was found to be between $5.7\text{-}1.6 \times$
 375 $10^{-6} \text{ cm}^2 \text{ s}^{-1}$.



376
 377 *Figure 7: Water diffusion coefficients of unaged (NA) cellulose acetate (CA) samples during (a) absorption and (b) desorption.*
 378 *D decreases with an increase of RH*

379 The results from this work show that D increases with an increase of plasticiser concentration (Figure
380 7). Because plasticisers disrupt polymer-polymer interactions, they can decrease the polymer's
381 crystallinity and therefore, the mobility of polymer chains increases, causing the increase of D. For
382 aged samples, we can suppose that D is more influenced by the loss of plasticiser, as plasticised
383 samples show a decrease of D after ageing and the un-plasticised aged and unaged samples do not
384 show significant differences in measured D values (Table S8 and S9, supplementary document). These
385 results are in contradiction with Belokurova et al. (2004) who have observed that D decreases when
386 plasticiser content is below 20 wt%, with plasticiser supposedly acting as an 'obstacle' to the water's
387 path. However, in that study the thickness of the samples varied from 0.02 to 0.05 mm and it is unclear
388 how D has been determined and at which RH.

389 A decrease in D with increased RH was also observed. This has been observed previously by Roussis
390 (1981a, 1981b) who explained that water absorption involves two phases: an initial fast phase where
391 the cavities are filled, followed by a slow absorption. The slow absorption is caused by a molecular
392 rearrangement of the system caused by the adsorption of water molecules onto each other, forming
393 clusters, behaviour typical of poor solvents such as water in relatively hydrophobic polymers (G. Q.
394 Chen et al., 2015; Roussis, 1981a). The phenomenon by which the presence of clusters decreases the
395 penetrant's diffusivity is known as 'antiplasticisation' (Chen et al., 2015; Favre et al., 1994; Hsu et al.,
396 1993; Pan et al., 2009; Takizawa et al., 1980). During desorption, a less significant increase in D can be
397 observed with the decrease in humidity, maintaining again the relationship between D and RH (Figure
398 6b).

399 3.3 Diethyl Phthalate loss

400 During the mass loss experiment performed at constant temperature and RH, only samples plasticised
401 with diethyl phthalate showed a significant loss of mass. The loss of plasticiser was confirmed by
402 SPME-GC/MS analysis where analysis of the VOCs emitted from the samples detected only a
403 compound whose mass spectrum contained peaks at m/z 177 possibly due to a loss of [OC₂H₅]; m/z
404 149 from the formation of protonated phthalic anhydride, and m/z 76, likely a fragmentation product
405 from the latter. These peaks are associated with the fragmentation of diethyl phthalate (Yin et al.,
406 2014). On the other hand, no characteristic peaks of triphenyl phosphate were observed during the
407 analysis of triphenyl phosphate-containing samples, indicating no loss of triphenyl phosphate into the
408 headspace of the sample at room temperature. This is to be expected, given that diethyl phthalate is
409 significantly more volatile than triphenyl phosphate, which is a solid at room temperature. Therefore,
410 this section is focused on the loss of diethyl phthalate.

411 The extent of the mass loss increases with an increase of temperature and of RH as shown by Figure
412 S6a (supplementary document), furthermore, the mass loss plotted against square root of time (Figure
413 S6b, supplementary document) does not show a linear dependence indicating that diethyl phthalate
414 loss under these conditions is governed by evaporation (Kovačić & Mrklič, 2002; Wei et al., 2019). It is
415 being assumed that all mass loss is due to diethyl phthalate loss, this is believed to be valid as the RH
416 was held constant for these experiments and the low temperatures mean that loss of volatiles due to
417 polymer degradation are likely to be negligible over the short timescales of the experiment. Further
418 discussion of the relationship between plasticiser loss and water uptake is given below.

419 The dependence of the rate of plasticiser loss on the residual mass of plasticiser (m_r) has been
420 described by the following ordinary differential equation (Kovačić & Mrklič, 2002; Lustoň et al., 1993;
421 Lustoň et al., 1993; Matsumoto, 1983; Mrklič et al., 2004; Mrklič & Kovačić, 1998):

$$422 \frac{dm}{dt} = -km \quad (5)$$

423 where m is the mass of plasticiser present in the sample at time t and k is the rate constant for
424 evaporative loss.

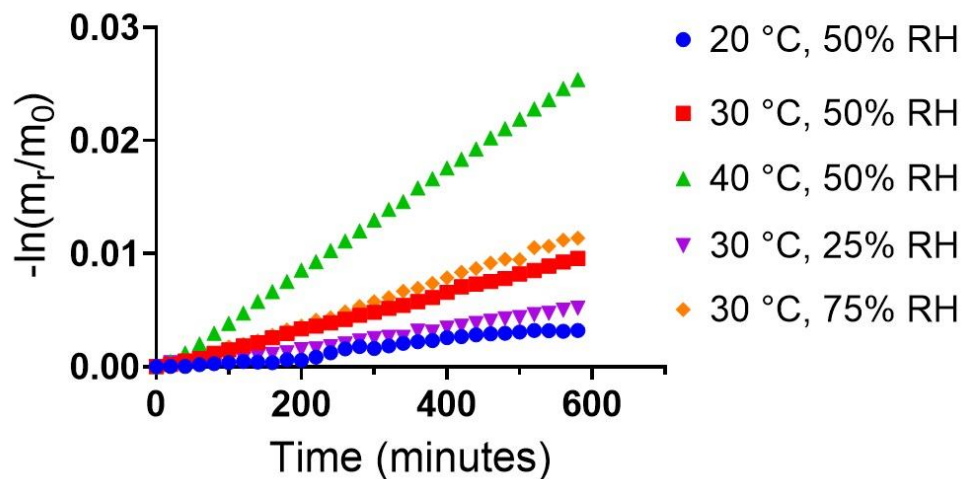
425 Integrating Equation 5 gives:

$$426 \quad m_r = m_0 e^{-kt} \quad (6)$$

427 where m_r is the residual mass of plasticiser left in the sample at time t , m_0 is the initial mass of
 428 plasticiser. Equation 6 can be linearized as:

$$429 \quad -\ln\left(\frac{m_r}{m_0}\right) = kt \quad (7)$$

430 Rate constants can be calculated using linear regression analysis from the slope obtained from the
 431 plot of $-\ln(m_r/m_0)$ against time (Figure 8).
 432



433
 434 *Figure 8: Plot of $-\ln(m_r/m_0)$ against time used to determine the rate constant of volatilisation k . m_r is the residual*
 435 *mass while m_0 represents the initial mass of plasticiser.*

436 During the experiments, some fluctuations appear at longer times. This is likely due to two processes.
 437 The first is the balance between water uptake and plasticiser loss. As the sample loses plasticiser, its
 438 affinity towards water vapour increases and therefore its water uptake also increases. This cycling
 439 between loss of diethyl phthalate and increase in water content, is most noticeable at a temperature
 440 of 20 °C. The second process is the effect of equipment temperature fluctuations and its impact on
 441 buoyancy forces which are more noticeable as the mass changes being measured are small.
 442 To reduce the impact these non-linearities have on the final results, the k parameters have been
 443 measured between 70 and ~500 min of the experiment where a constant rate of mass loss has been
 444 observed. The measured values of k are shown in Table 1.
 445

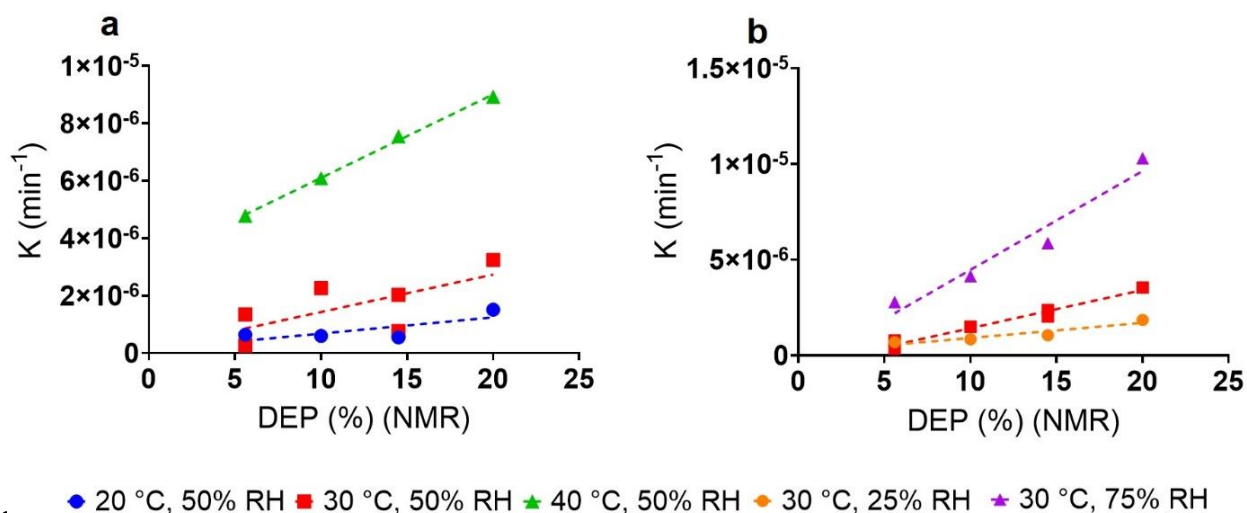
446 *Table 1: Rate constant of evaporation (k) of diethyl phthalate (DEP) at different temperatures and relative*
 447 *humidity.*

DEP (%) ¹ H NMR	k ($\times 10^{-6} \text{ min}^{-1}$)				
	20 °C, 50% RH	30 °C, 50% RH	40 °C, 50% RH	30 °C, 25% RH	30 °C, 75% RH
5.6 ± 0.67	0.42 ± 2.06 · 10 ⁻³	0.56 ± 4.66 · 10 ^{-3*}	4.89 ± 7 · 10 ⁻³	0.69 ± 2.31 · 10 ⁻³	2.78 ± 1.4 · 10 ⁻²
10.3	0.55 ± 3.52 · 10 ⁻³	1.49 ± 1.84 · 10 ⁻³	6.27 ± 5.5 · 10 ⁻³	0.84 ± 3.48 · 10 ⁻³	4.14 ± 3.7 · 10 ⁻³
14.5 ± 1.55	0.62 ± 1.70 · 10 ⁻³	2.20 ± 2.2 · 10 ^{-3*}	7.79 ± 3.7 · 10 ⁻³	1.05 ± 4.48 · 10 ⁻³	5.86 ± 7.2 · 10 ⁻³
19.8	1.36 ± 7.83 · 10 ⁻³	3.53 ± 3.04 · 10 ⁻³	8.96 ± 3.7 · 10 ⁻³	1.85 ± 464 · 10 ⁻³	10.3 ± 4.1 · 10 ⁻³

448 *data from duplicates

449 Equations 5-7 assume an evaporation coefficient (k) that is independent of the concentration of
 450 plasticiser. Given the linearity of the traces in Figure 8 and in Figure S6a of the supplementary
 451 information, we believe this assumption to be valid for the small mass losses that occurred in these
 452 experiments. However, when samples with different initial concentrations of plasticiser are used, it is
 453 possible to observe a dependence of k on the initial concentration (Figure 9). This dependence has
 454 also been observed by others during thermogravimetric analysis (Kovačić & Mrklič, 2002; Mrklič et al.,
 455 2004; Mrklič & Kovačić, 1998) where k displayed a linear dependence on initial plasticiser
 456 concentration.

457 As k is dependent on m_0 we can confirm again, that in these experiments the loss of diethyl phthalate
 458 from cellulose acetate films is evaporation controlled and its dependence on temperature and RH is
 459 evident (Figure 9).



460 ● 20 °C, 50% RH ■ 30 °C, 50% RH ▲ 40 °C, 50% RH ◆ 30 °C, 25% RH ★ 30 °C, 75% RH
 461 Figure 9: Rate constant of evaporation (k) of different plasticiser concentration at different temperature (a) and
 462 RH (b). Both graphs show that k is dependent on initial concentration, temperature and RH.
 463

464 This work illustrates how both water diffusion and plasticiser depend on both the chemical
 465 composition of cellulose acetate and environmental factors (such as temperature and RH). This work
 466 represents a significant contribution to our understanding of the interactions between water and
 467 cellulose acetate. While several previous works have demonstrated the correlation between DS and
 468 the sorption and diffusion of water, these studies are often on membranes, rather than plastics and
 469 with the exception of the work by Belokurova et al. (2004), do not explore the effect of
 470 plasticiser. Plasticisers are important additives in cellulose acetate production and are very commonly
 471 found in cellulose acetate objects. An understanding of the way in which plasticisers affect the
 472 behaviour of water in cellulose acetate is therefore critical in understanding cellulose acetate-water
 473 interactions.

474 Furthermore, we provide insight into how different physical and chemical degradation mechanisms
 475 interact with each other in cellulose acetate. We have shown that loss of plasticiser causes an increase
 476 in the hydrophilicity of cellulose acetate. This will lead to increased uptake of water which in turn will
 477 increase the rates of other decay mechanisms such as deacetylation and chain scission. This is an
 478 important insight for museums who work with plastic collections. Our work provides a more in-depth
 479 analysis of the inter-connection between plasticiser loss and hydrolysis degradation reactions in
 480 cellulose acetate than has previously been seen in the literature.

481 This work also demonstrates the usefulness of DVS as a technique for understanding material
482 properties in a cultural heritage context. The relationships between material properties, changes in
483 RH and water content is very relevant to the study of many heritage materials, including wood, textiles
484 and paper. This article demonstrates the insight that DVS can provide into these relationships.

485 **4 Conclusion**

486 In this study, the transport phenomena of water and plasticisers in cellulose acetate film at ambient
487 conditions have been investigated and the following can be concluded:

- 488 • With an increase of plasticiser concentration cellulose acetate absorbs less water. Due to
489 plasticiser loss during ageing the material becomes more hydrophilic.
- 490 • Hysteresis decreases with the increases of plasticisers. This is due to higher water content
491 during desorption process, which can cause other decay processes such as deacetylation and
492 chain scission.
- 493 • The diffusion coefficient of water (D) decreases with an increase in RH possibly caused by the
494 formation of clusters of water, a phenomenon known as ‘antiplasticisation’.
- 495 • D increases with the increase of plasticiser concentration which causes reduced crystallinity
496 and therefore enhances the chain mobility, facilitating the diffusion of water within the
497 sample.
- 498 • During the mass loss experiment only samples containing diethyl phthalate plasticiser showed
499 mass loss as confirmed by SPME analysis
- 500 • The evaporative loss of diethyl phthalate is dependent on the initial concentration of
501 plasticiser, RH and temperature.
502

503 **Declaration of Competing Interest**

504 The authors declare no competing financial interests or personal relationships that could have
505 appeared to influence the work reported in this paper.

506 **Acknowledgement**

507 This project has received funding from the European Research Council (ERC) under the European
508 Union's Horizon 2020 research and innovation programme (grant agreement no 716390). We would
509 like to thank Dr. John Duncan from Lacerta technology (UK) and Abby Moore from the Museum of
510 London (UK) for their support. We would like to thank Dr. Abil Aliev from UCL Chemistry (UK) as well
511 for his help for NMR spectroscopy.

512 **Reference**

- 513 Alamri, M. S., Mohamed, A. A., Hussain, S., Ibraheem, M. A., & Abdo Qasem, A. A. (2018).
514 Determination of Moisture Sorption Isotherm of Crosslinked Millet Flour and Oxirane
515 Using GAB and BET. *Journal of Chemistry*, 2018, e2369762.
516 <https://doi.org/10.1155/2018/2369762>
- 517 Allada, R., Maruthapillai, A., Palanisamy, K., & Chappa, P. (2017). Moisture Sorption–
518 desorption Characteristics and the Corresponding Thermodynamic Properties of
519 Carvedilol Phosphate. *Journal of Pharmacy & Bioallied Sciences*, 9(1), 16–21.
520 <https://doi.org/10.4103/0975-7406.206216>
- 521 Allen, N., Edge, M., Appleyard, J. H., Jewitt, T. S., Horie, C. V., & FRANCIS, D. (1987).
522 Degradation of historic cellulose triacetate cinematographic film: The vinegar

523 syndrome. *Polymer Degradation and Stability*, 19, 379–387.
524 [https://doi.org/10.1016/0141-3910\(87\)90038-3](https://doi.org/10.1016/0141-3910(87)90038-3)

525 Argyropoulos, D., Alex, R., & Müller, J. (2011). Equilibrium moisture contents of a
526 medicinal herb (*Melissa officinalis*) and a medicinal mushroom (*Lentinula edodes*)
527 determined by dynamic vapour sorption. *Procedia Food Science*, 1, 165–172.
528 <https://doi.org/10.1016/j.profoo.2011.09.026>

529 Asai, T., Taniguchi, H., Kinoshita, E., & Nakamura, K. (2001). Thermal and mechanical
530 properties of cellulose acetates with various degrees of acetylation in dry and wet states.
531 In *Recent Advances in Environmentally Compatible Polymers* (pp. 275–280). Elsevier.
532 <https://doi.org/10.1533/9781845693749.5.275>

533 Ballany, J., Littlejohn, D., Pethrick, R. A., & Quye, A. (2000). Probing the Factors That
534 Control Degradation in Museum Collections of Cellulose Acetate Artefacts. In J. M.
535 Cardamone & M. T. Baker (Eds.), *Historic Textiles, Papers, and Polymers in Museums*
536 (Vol. 779, pp. 145–165). American Chemical Society. <https://doi.org/10.1021/bk-2001-0779.ch012>

537 Barham, A. S., Tewes, F., & Healy, A. M. (2015). Moisture diffusion and permeability
538 characteristics of hydroxypropylmethylcellulose and hard gelatin capsules. *International*
539 *Journal of Pharmaceutics*, 478(2), 796–803.
540 <https://doi.org/10.1016/j.ijpharm.2014.12.029>

541 Belokurova, A. P., Burmistrov, V. A., Chalykh, A. E., & Koifman, O. I. (2004). Diffusion
542 and dissolution of water vapour in plasticised cellulose acetates. *International Polymer*
543 *Science and Technology*, 32(11), 63–66. <https://doi.org/10.1177/0307174X0503200213>

544 Brydson, J. A. (1999). 22—Cellulose Plastics. In *Plastics Materials (Seventh Edition)* (pp.
545 613–634). Butterworth-Heinemann.
546 <http://www.sciencedirect.com/science/article/pii/B9780750641326500632>

547 Cao, Y., Zhang, J., He, J., Li, H., & Zhang, Y. (2010). Homogeneous Acetylation of
548 Cellulose at Relatively High Concentrations in an Ionic Liquid. *Chinese Journal of*
549 *Chemical Engineering*, 18(3), 515–522. [https://doi.org/10.1016/S1004-9541\(10\)60252-](https://doi.org/10.1016/S1004-9541(10)60252-2)
550 [2](https://doi.org/10.1016/S1004-9541(10)60252-2)

551 Céline, A., Gonçalves, O., Jacquemin, F., & Fréour, S. (2014). Qualitative and quantitative
552 assessment of water sorption in natural fibres using ATR-FTIR spectroscopy.
553 *Carbohydrate Polymers*, 101, 163–170. <https://doi.org/10.1016/j.carbpol.2013.09.023>

554 Chen, G. Q., Kanehashi, S., Doherty, C. M., Hill, A. J., & Kentish, S. E. (2015). Water vapor
555 permeation through cellulose acetate membranes and its impact upon membrane
556 separation performance for natural gas purification. *Journal of Membrane Science*, 487,
557 249–255. <https://doi.org/10.1016/j.memsci.2015.03.074>

558 Chen, M., Coasne, B., Guyer, R., Derome, D., & Carmeliet, J. (2018). Role of hydrogen
559 bonding in hysteresis observed in sorption-induced swelling of soft nanoporous
560 polymers. *Nature Communications*, 9(1), 1–7. [https://doi.org/10.1038/s41467-018-](https://doi.org/10.1038/s41467-018-05897-9)
561 [05897-9](https://doi.org/10.1038/s41467-018-05897-9)

562 Crank, J. (1975). *The mathematics of diffusion* (2d ed). Clarendon Press.

563 Curran, K., Underhill, M., Gibson, L. T., & Strlic, M. (2016). The development of a SPME-
564 GC/MS method for the analysis of VOC emissions from historic plastic and rubber
565 materials. *Microchemical Journal*, 124, 909–918.
566 <https://doi.org/10.1016/j.microc.2015.08.027>

567 Da Ros, S., Aliev, A. E., del Gaudio, I., King, R., Pokorska, A., Kearney, M., & Curran, K.
568 (2020). Characterising plasticised cellulose acetate-based historic artefacts by NMR
569 spectroscopy: A new approach for quantifying the degree of substitution and diethyl
570 phthalate contents. *Polymer Degradation and Stability*, 109420.
571 <https://doi.org/10.1016/j.polymdegradstab.2020.109420>

573 Edge, M., Allen, N. S., Jewitt, T. S., & Horie, C. V. (1989a). Fundamental aspects of the
574 degradation of cellulose triacetate base cinematograph film. *Polymer Degradation and*
575 *Stability*, 25(2–4), 345–362. [https://doi.org/10.1016/S0141-3910\(89\)81016-X](https://doi.org/10.1016/S0141-3910(89)81016-X)

576 Edwards, H. G. M., Johnson, A. F., Lewis, I. R., & Turner, P. (1993a). Raman spectroscopic
577 studies of ‘Pedigree Doll disease’. *Polymer Degradation and Stability*, 41(3), 257–264.
578 [https://doi.org/10.1016/0141-3910\(93\)90072-Q](https://doi.org/10.1016/0141-3910(93)90072-Q)

579 Farris, S., Introzzi, L., Biagioni, P., Holz, T., Schiraldi, A., & Piergiovanni, L. (2011).
580 Wetting of Biopolymer Coatings: Contact Angle Kinetics and Image Analysis
581 Investigation. *Langmuir*, 27(12), 7563–7574. <https://doi.org/10.1021/la2017006>

582 Favre, E., Schaetzel, P., Nguyen, Q. T., Clément, R., & Néel, J. (1994). Sorption, diffusion
583 and vapor permeation of various penetrants through dense poly(dimethylsiloxane)
584 membranes: A transport analysis. *Journal of Membrane Science*, 92(2), 169–184.
585 [https://doi.org/10.1016/0376-7388\(94\)00060-3](https://doi.org/10.1016/0376-7388(94)00060-3)

586 Gautam, V., Srivastava, A., Singh, K. P., & Yadav, V. L. (2016). Vibrational and gravimetric
587 analysis of polyaniline/polysaccharide composite materials. *Polymer Science Series A*,
588 58(2), 206–219. <https://doi.org/10.1134/S0965545X16020085>

589 Godwin, A. D. (2017). Plasticizers. In *Applied Plastics Engineering Handbook* (pp. 533–
590 553). Elsevier. <https://doi.org/10.1016/B978-0-323-39040-8.00025-0>

591 Hsu, W. P., Li, R. J., Myerson, A. S., & Kwei, T. K. (1993). Sorption and diffusion of water
592 vapour in hydrogen-bonded polymer blends. *Polymer*, 34(3), 597–603.
593 [https://doi.org/10.1016/0032-3861\(93\)90556-P](https://doi.org/10.1016/0032-3861(93)90556-P)

594 Hunter-Sellars, E., Tee, J. J., Parkin, I. P., & Williams, D. R. (2020). Adsorption of volatile
595 organic compounds by industrial porous materials: Impact of relative humidity.
596 *Microporous and Mesoporous Materials*, 298, 110090.
597 <https://doi.org/10.1016/j.micromeso.2020.110090>

598 Kalaycıoğlu, Z., Kahya, N., Adımcılar, V., Kaygusuz, H., Torlak, E., Akin-Evingür, G., &
599 Erim, F. B. (2020). Antibacterial nano cerium oxide/chitosan/cellulose acetate
600 composite films as potential wound dressing. *European Polymer Journal*, 133, 109777.
601 <https://doi.org/10.1016/j.eurpolymj.2020.109777>

602 Karbowski, T., Debeaufort, F., Champion, D., & Voilley, A. (2006). Wetting properties at the
603 surface of iota-carrageenan-based edible films. *Journal of Colloid and Interface*
604 *Science*, 294(2), 400–410. <https://doi.org/10.1016/j.jcis.2005.07.030>

605 Keely, C. M., Zhang, X., & McBrierty, V. J. (1995). Hydration and plasticization effects in
606 cellulose acetate: A solid-state NMR study. *Journal of Molecular Structure*, 355(1), 33–
607 46. [https://doi.org/10.1016/0022-2860\(95\)08865-S](https://doi.org/10.1016/0022-2860(95)08865-S)

608 Kohler, R., Dück, R., Ausperger, B., & Alex, R. (2003). A numeric model for the kinetics of
609 water vapor sorption on cellulosic reinforcement fibers. *Composite Interfaces*, 10(2–3),
610 255–276. <https://doi.org/10.1163/156855403765826900>

611 Kokoszka, S., Debeaufort, F., Hambleton, A., Lenart, A., & Voilley, A. (2010). Protein and
612 glycerol contents affect physico-chemical properties of soy protein isolate-based edible
613 films. *Innovative Food Science & Emerging Technologies*, 11(3), 503–510.
614 <https://doi.org/10.1016/j.ifset.2010.01.006>

615 Kovačić, T., & Mrklič, Ž. (2002). The kinetic parameters for the evaporation of plasticizers
616 from plasticized poly(vinyl chloride). *Thermochimica Acta*, 381(1), 49–60.
617 [https://doi.org/10.1016/S0040-6031\(01\)00643-8](https://doi.org/10.1016/S0040-6031(01)00643-8)

618 Kurokawa, Y. (1981). Adsorption of water on cellulose acetate membrane. *Desalination*,
619 36(3), 285–290. [https://doi.org/10.1016/S0011-9164\(00\)88645-2](https://doi.org/10.1016/S0011-9164(00)88645-2)

620 Kymäläinen, M., Rautkari, L., & Hill, C. A. S. (2015). Sorption behaviour of torrefied wood
621 and charcoal determined by dynamic vapour sorption. *Journal of Materials Science*,
622 50(23), 7673–7680. <https://doi.org/10.1007/s10853-015-9332-2>

- 623 Lattuati-Derieux, A., Egasse, C., Thao-Heu, S., Balcar, N., Barabant, G., & Lavédrine, B.
624 (2013). What do plastics emit? HS-SPME-GC/MS analyses of new standard plastics and
625 plastic objects in museum collections. *Journal of Cultural Heritage*, 14(3), 238–247.
626 <https://doi.org/10.1016/j.culher.2012.06.005>
- 627 Leão, T. P., & Tuller, M. (2014). Relating soil specific surface area, water film thickness, and
628 water vapor adsorption. *Water Resources Research*, 50(10), 7873–7885.
629 <https://doi.org/10.1002/2013WR014941>
- 630 Littlejohn, D., Pethrick, R. A., Quye, A., & Ballany, J. M. (2013). Investigation of the
631 degradation of cellulose acetate museum artefacts. *Polymer Degradation and Stability*,
632 98(1), 416–424. <https://doi.org/10.1016/j.polymdegradstab.2012.08.023>
- 633 Lonsdale, H. K., Merten, U., & Riley, R. L. (1965). Transport properties of cellulose acetate
634 osmotic membranes. *Journal of Applied Polymer Science*, 9(4), 1341–1362.
635 <https://doi.org/10.1002/app.1965.070090413>
- 636 Lustoñ, J., Pastušáková, V., & Vašš, F. (1993). Effect of phase transitions on the volatility of
637 UV absorbers from polypropylene. *Journal of Applied Polymer Science*, 47(3), 555–
638 562. <https://doi.org/10.1002/app.1993.070470315>
- 639 Lustoñ, J., Pastušáková, V., & Vašš, F. (1993). Volatility of additives from polymers.
640 Concentration dependence and crystallinity effects. *Journal of Applied Polymer Science*,
641 48(2), 219–224. <https://doi.org/10.1002/app.1993.070480205>
- 642 Macro, N. (2019). *The paradox of conserving plastic: A contemporary challenge* (pp 141-
643 155). Università degli studi dell'Aquila.
- 644 Matsumoto, S. (1983). Behavior of antioxidant in polyethylene. *Journal of Polymer Science:*
645 *Polymer Chemistry Edition*, 21(2), 557–564.
646 <https://doi.org/10.1002/pol.1983.170210222>
- 647 McGath, M. K. (2012). *Investigation of deterioration mechanisms of cellulose acetate*
648 *compounded with triphenyl phosphate* (pp. 20–31). University of Arizona.
- 649 Modaressi, H., & Garnier, G. (2002). Mechanism of Wetting and Absorption of Water
650 Droplets on Sized Paper: Effects of Chemical and Physical Heterogeneity. *Langmuir*,
651 18(3), 642–649. <https://doi.org/10.1021/la0104931>
- 652 Mrklič, Ž., & Kovačić, T. (1998). Thermogravimetric investigation of volatility of dioctyl
653 phthalate from plasticized poly(vinyl chloride). *Thermochimica Acta*, 322(2), 129–135.
654 [https://doi.org/10.1016/S0040-6031\(98\)00479-1](https://doi.org/10.1016/S0040-6031(98)00479-1)
- 655 Mrklič, Ž., Rušić, D., & Kovačić, T. (2004). Kinetic model of the evaporation process of
656 benzylbutyl phthalate from plasticized poly(vinyl chloride). *Thermochimica Acta*,
657 414(2), 167–175. <https://doi.org/10.1016/j.tca.2003.12.010>
- 658 Murphy, D., & de Pinho, M. N. (1995). An ATR-FTIR study of water in cellulose acetate
659 membranes prepared by phase inversion. *Journal of Membrane Science*, 106(3), 245–
660 257. [https://doi.org/10.1016/0376-7388\(95\)00089-U](https://doi.org/10.1016/0376-7388(95)00089-U)
- 661 Oberbossel, G., Zihlmann, S., Roth, C., & Rohr, P. R. von. (2016). Contact Angle Decay
662 Model to Study Plasma Afterglow Activation of Polymers. *Plasma Processes and*
663 *Polymers*, 13(9), 937–945. <https://doi.org/10.1002/ppap.201600022>
- 664 Okubayashi, S., Griesser, U., & Bechtold, T. (2004). A kinetic study of moisture sorption and
665 desorption on lyocell fibers. *Carbohydrate Polymers*, 58(3), 293–299.
666 <https://doi.org/10.1016/j.carbpol.2004.07.004>
- 667 Palin, M. J., Gittens, G. J., & Porter, G. B. (1975). Determination of diffusion coefficients of
668 water in cellulose acetate membranes. *Journal of Applied Polymer Science*, 19(4),
669 1135–1146. <https://doi.org/10.1002/app.1975.070190421>
- 670 Pan, F., Ma, J., Cui, L., & Jiang, Z. (2009). Water vapor/propylene sorption and diffusion
671 behavior in PVA–P(AA-AMPS) blend membranes by GCMC and MD simulation.

672 *Chemical Engineering Science*, 64(24), 5192–5197.
673 <https://doi.org/10.1016/j.ces.2009.08.026>

674 Park, H.-M., Liang, X., Mohanty, A. K., Misra, M., & Drzal, L. T. (2004). Effect of
675 Compatibilizer on Nanostructure of the Biodegradable Cellulose Acetate/Organoclay
676 Nanocomposites. *Macromolecules*, 37(24), 9076–9082.
677 <https://doi.org/10.1021/ma048958s>

678 Park, H.-M., Misra, M., Drzal, L. T., & Mohanty, A. K. (2004). “Green” Nanocomposites
679 from Cellulose Acetate Bioplastic and Clay: Effect of Eco-Friendly Triethyl Citrate
680 Plasticizer. *Biomacromolecules*, 5(6), 2281–2288. <https://doi.org/10.1021/bm049690f>

681 Popescu, C.-M., Hill, C. A. S., & Kennedy, C. (2016). Variation in the sorption properties of
682 historic parchment evaluated by dynamic water vapour sorption. *Journal of Cultural
683 Heritage*, 17, 87–94. <https://doi.org/10.1016/j.culher.2015.06.001>

684 Preda, F. M., Alegría, A., Bocahut, A., Fillot, L. A., Long, D. R., & Sotta, P. (2015).
685 Investigation of Water Diffusion Mechanisms in Relation to Polymer Relaxations in
686 Polyamides. *Macromolecules*. <https://doi.org/10.1021/acs.macromol.5b01295>

687 Rajabnezhad, S., Ghafourian, T., Rajabi-Siahboomi, A., Missaghi, S., Naderi, M., Salvage, J.
688 P., & Nokhodchi, A. (2020). Investigation of water vapour sorption mechanism of
689 starch-based pharmaceutical excipients. *Carbohydrate Polymers*, 238, 116208.
690 <https://doi.org/10.1016/j.carbpol.2020.116208>

691 Rhim, J.-W., & Ng, P. K. W. (2007). Natural Biopolymer-Based Nanocomposite Films for
692 Packaging Applications. *Critical Reviews in Food Science and Nutrition*, 47(4), 411–
693 433. <https://doi.org/10.1080/10408390600846366>

694 Richardson, E., Truffa Giachet, M., Schilling, M., & Learner, T. (2014). Assessing the
695 physical stability of archival cellulose acetate films by monitoring plasticizer loss.
696 *Polymer Degradation and Stability*, 107, 231–236.
697 <https://doi.org/10.1016/j.polymdegradstab.2013.12.001>

698 Roussis, P. P. (1981a). Diffusion of water vapour in cellulose acetate: 1. Differential transient
699 sorption kinetics and equilibria. *Polymer*, 22(6), 768–773. [https://doi.org/10.1016/0032-3861\(81\)90012-4](https://doi.org/10.1016/0032-3861(81)90012-4)

700

701 Roussis, P. P. (1981b). Diffusion of water vapour in cellulose acetate: 2. Permeation and
702 integral sorption kinetics. *Polymer*, 22(8), 1058–1063. [https://doi.org/10.1016/0032-3861\(81\)90292-5](https://doi.org/10.1016/0032-3861(81)90292-5)

703

704 Scandola, M., & Ceccorulli, G. (1985). Viscoelastic properties of cellulose derivatives: 2.
705 Effect of diethylphthalate on the dynamic mechanical relaxations of cellulose acetate.
706 *Polymer*, 26(13), 1958–1962. [https://doi.org/10.1016/0032-3861\(85\)90174-0](https://doi.org/10.1016/0032-3861(85)90174-0)

707 Sharma, A., Mandal, T., & Goswami, S. (2021). Fabrication of cellulose acetate
708 nanocomposite films with lignocellulosic nanofiber filler for superior effect on thermal,
709 mechanical and optical properties. *Nano-Structures & Nano-Objects*, 25, 100642.
710 <https://doi.org/10.1016/j.nanoso.2020.100642>

711 Shashoua, Y. (2008). *Conservation of plastics: Materials science, degradation and
712 preservation* (1st ed, pp. 159-161, 180-184). Elsevier/Butterworth-Heinemann.

713 Shashoua, Y. (2014). A Safe Place Storage Strategies for Plastics. *The GCI Newsletter,
714 Conservation Perspectives Spring*, 29(1), 13–15.

715 Skorniyakov, I. V., & Komar, V. P. (1998). IR spectra and the structure of plasticized
716 cellulose acetate films. *Journal of Applied Spectroscopy*, 65(6), 911–918.
717 <https://doi.org/10.1007/BF02675748>

718 Solaro, R., Chiellini, F., & Battisti, A. (2010). Targeted Delivery of Protein Drugs by
719 Nanocarriers. *Materials*, 3(3), 1928–1980. <https://doi.org/10.3390/ma3031928>

720 Takahashi, K., Sasaki, M., Hayakawa, H., Yajima, H., & Oda, Y. (2021). Composition of the
721 white precipitate formed on the surface of damaged triacetyl cellulose-based motion

722 picture films. *Scientific Reports*, 11(1), 1502. [https://doi.org/10.1038/s41598-020-](https://doi.org/10.1038/s41598-020-80498-5)
723 80498-5

724 Takizawa, A., Kinoshita, T., Sasaki, M., & Tsujita, Y. (1980). Solubility and diffusion of
725 binary water—Methyl alcohol vapor mixtures in cellulose acetate membranes. *Journal*
726 *of Membrane Science*, 6, 265–269. [https://doi.org/10.1016/S0376-7388\(00\)82168-7](https://doi.org/10.1016/S0376-7388(00)82168-7)

727 Wäntig, F. (2008). *Plastics in Art: A Study from the Conservation Point of View* (pp. 216-
728 222). Imhof.

729 Wei, X.-F., Linde, E., & Hedenqvist, M. S. (2019). Plasticiser loss from plastic or rubber
730 products through diffusion and evaporation. *Npj Materials Degradation*, 3(1), 1–8.
731 <https://doi.org/10.1038/s41529-019-0080-7>

732 Xie, Y., Hill, C. A. S., Jalaludin, Z., Curling, S. F., Anandjiwala, R. D., Norton, A. J., &
733 Newman, G. (2011). The dynamic water vapour sorption behaviour of natural fibres and
734 kinetic analysis using the parallel exponential kinetics model. *Journal of Materials*
735 *Science*, 46(2), 479–489. <https://doi.org/10.1007/s10853-010-4935-0>

736 Yin, P., Chen, H., Liu, X., Wang, Q., Jiang, Y., & Pan, R. (2014). Mass Spectral
737 Fragmentation Pathways of Phthalate Esters by Gas Chromatography–Tandem Mass
738 Spectrometry. *Analytical Letters*, 47(9), 1579–1588.
739 <https://doi.org/10.1080/00032719.2013.879658>

740 Zhang, X.-R., Zhang, L.-Z., & Pei, L.-X. (2013). Sorption, permeation and selective transport
741 of moisture/VOCs through a CA membrane for total heat recovery. *International*
742 *Journal of Low-Carbon Technologies*, 8(1), 64–69. <https://doi.org/10.1093/ijlct/cts022>
743